arXiv:2605.15951v1 [cs.CV] 15 May 2026

From Failure to Feedback: Group Revision Unlocks Hard Cases in Object-Level Grounding

Yuyuan Liu [1] Yiping Ji [2] Anjie Le [1] Jiayuan Zhu [1] Jiazhen Pan [3]
Can Peng [1] Jiajun Deng [4] Fengbei Liu [5](✉) Junde Wu [1]

[1] Department of Engineering Science, University of Oxford [2] Australian Institute for Machine Learning, Adelaide University
[3] Technical University of Munich [4] University of Science and Technology of China [5] Cornell University

Abstract

Finetuning Large Vision-Language Models with reinforcement learning has emerged as a promising approach to enhance their capability in object-level grounding. However, existing methods, mainly based on GRPO, assign rewards at the response level. Such sparse reward, often criterion-induced, leads to minimal learning signals when all candidate responses fail in challenging scenarios. In this work, we propose a group-revision optimisation paradigm that enhances learning on hard cases. It begins with a sampled initial response and generates a set of revised candidates to explore improved grounding outcomes. Inspired by reward shaping, we introduce a consolidation process that quantifies each candidate's improvement over the initial attempt and converts it into informative shaping signals. These signals are used to both refine the reward and modulate the advantage, amplifying the influence of high-quality revisions. Our method achieves consistent gains across referring and reasoning segmentation, REC, and counting benchmarks compared with prior GRPO-based models. Our code is available at https://github.com/yyliu01/GroupRevision.

1. Introduction

Large Vision–Language Models (LVLMs) [3, 16, 75] have made significant advances in multimodal reasoning. From open-ended scene summarisation [39, 46, 104] to content-based retrieval [11, 80], they have demonstrated strong performance in general image understanding. Yet, when questions target specific objects within an image, such as their *location*, LVLMs often struggle to ground answers precisely [30, 36, 67]. This reveals a broader limitation: current models fail to fully exploit the *object-level* grounding signals present in the scene [27, 47, 72], rather than general visual reasoning. As a result, in tasks such as embodied navigation [63, 74, 79], robotic manipulation [28, 98, 100], and clinical imaging [33], where both reasoning and object-level grounding are required, current LVLMs still fall short in delivering reliable performance.

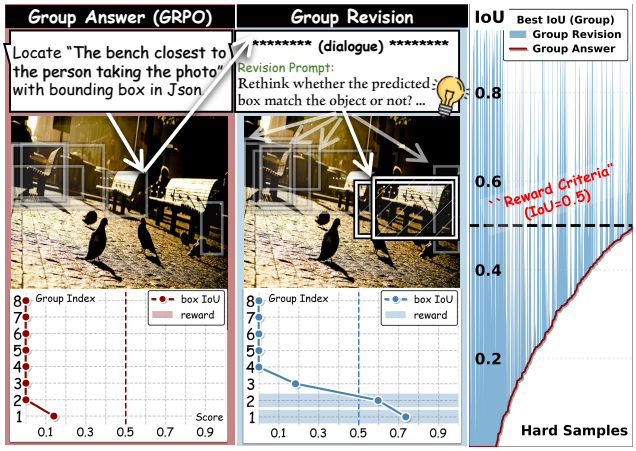

Figure 1. **Group Answer (GRPO)**: A group of responses (n=8) from Qwen2.5VL-7B [3] yields unsatisfactory grounding, with the best box IoU only 14.72%. **Group Revision**: A group of responses that revises the mistaken answer improves the best IoU to 74.57%. **Quantitative study:** The red curve shows the best IoU within each GRPO group on the hard cases through the training set, while the group revision effectively recover the reward signal.

A promising direction to bridge this grounding gap is to fine-tune LVLMs using object-level reward signal via Group Relative Policy Optimisation (GRPO) [68]. For a image-question pair, the policy samples a group of candidate responses, each scored based on whether it correctly localises the target object. The policy is then updated to increase the likelihood of higher-reward outputs. In this vein, early efforts [50, 52, 70] trained LVLMs to predict object bounding boxes for detection [52] or referring expression comprehension (REC) [70], and to generate points (inside the object) that guide SAM2 [65] in producing segmentation masks [29, 89]. Recent work [51] further shows that this training paradigm consistently improves performance on downstream tasks [35, 58] in multi-object scenarios.

Despite this progress, these GRPO-based methods still struggles to identify objects in complex scenes, especially when resolving references to similar-looking instances or interpreting fine-grained spatial relations. This mainly

stems from their optimisation process: when challenging examples lead all responses in the group to fail the reward criterion, the policy receives minimal training signal, leaving these hard cases unlearned. This failure mode arises from GRPO's sparse reward design [44, 55, 99], where only the final output is evaluated, and no reward or guidance is given for the intermediate decision that leads to it. Similar limitations have been observed in code generation [17, 41] and math reasoning [99], motivating the development of Process Reward Models (PRMs) [101] that deliver feedback at each step toward the solution. However, applying such step-wise reward to object-level visual grounding is challenging. It is non-trivial to link each intermediate reasoning sentence in the model's Chain-of-Thought (CoT) to a concrete object in the image that can provide learning feedback. This leads to a fundamental chicken-and-egg dilemma: the model needs more accurate intermediate guidance to obtain informative rewards, but these rewards are essential for learning to reason in the first place.

Yet, a failed attempt doesn't have to be the end—but a clue. Although explicit step-wise feedback is unavailable, failed attempts often reveal what the model missed. In such cases, revising the failure and exploring alternative responses can guide the model to attend to previously overlooked visual cues. As illustrated in Fig. 1, a directly sampled **GRPO** group fails to correctly localise the referent. In this case, we wrap one failed response with a follow-up revision prompt and sample a group of revised responses based on it. This **revision process** helps the model reinterpret the scene, allowing two candidates successfully localise the target. Importantly, such revision transforms a previously unrewarded case into one that satisfies the standard success criterion (e.g., box_IoU > 0.5 [50–52]), allowing it to contribute to training. This case is not isolated. The red curve in Fig. 1 **(Quantitative study)** highlights hard training samples that receive no supervision signal from a group of responses and remain unlearned from GRPO. After applying group revision, many of these samples recover reward. The majority of improve above the IoU cutoff, indicating consistent benefits across the dataset from the revised results.

While the revision group often yields better responses, they are evaluated independently of the initial failure. As a result, the policy receives no credit assignment for what actually changed to fix the error. Without this connection, the model treats each outcome as isolated, missing the opportunity to learn what improvements truly mattered. To bridge this gap, a consolidation process is needed to turn these improvements into measurable learning signals. It enables the model not just to retry, but to learn *why it succeeds after failing*. By internalising such improvements, the model can ultimately produce more accurate grounding results.

In this work, we introduce a group revision optimisation paradigm that enables LVLMs to recover training signal from challenging hard cases. Unlike prior methods that sample responses to answer the query, our approach forms a candidate group to collaboratively revise an earlier response. To achieve this, we first sample a single response from the policy given a image–question pair. We then generate a revision group conditioned on this response, aiming to better localise ambiguous or hard-to-detect objects. To transfer the gains from group revision into learnable training signals, we introduce a consolidation process inspired by reward shaping [14, 56, 78]. In this process, we compute an alignment cost that quantifies how much the revision improves upon the initial response, relative to the ground-truth objects. This alignment cost is then converted into a shaping signal that assigns finer-grained rewards within the revision group, allowing the model to identify which candidates are truly helpful. We further modulate the advantage with this shaping signal, so that informative candidates have a stronger impact on learning. As a result, the model is better guided to internalise improvements from revision, leading to more effective learning from difficult cases. In summary, we make the following core contributions:

- We propose a group-revision training paradigm, which revises an initial attempt through a group of responses, to unlock learning signals from hard cases in LVLMs;
- Within this strategy, we propose a consolidation process to quantify improvements over the initial output, resulting in a shaping signal used to construct the rewards; and
- This signal is further used to scale the advantage, boosting the contribution of informative candidates in training.

We evaluate our method on multiple visual perception tasks and observe robust improvements over GRPO-based state-of-the-art (SoTA) methods. Notably, our approach achieves average gains of +2.16% [35] on reasoning segmentation, +2.22% on referring segmentation [90], as well as +4.27% on object counting [18, 58] tasks.

2. Related work

Large Vision-Language Models (LVLMs) (also known as Multimodal Large Language Models) first gained attention with Flamingo [1] by DeepMind, which injects sampled visual tokens into the hidden layers of a frozen language model. For the first time, this enabled a language model to engage in image-grounded conversations. Motivated by this insight, subsequent works [21, 26, 104] either align visual and language tokens using pretrained transformer-based adapters [21, 26, 40, 104], or map CLIP-derived features into the language embedding space via visual instruction tuning [3, 13, 46, 75, 76, 105]. Despite their strong general performance, LVLMs often struggle with instance-level queries [8, 47, 67]. They tend to hallucinate details [30, 36], and fail to generate accurate, object-aligned outputs (e.g., masks or boxes) for the referenced entities. These issues remain a well-known obstacle to deploying LVLMs in tasks

that demand precise visual perception [6, 28, 49, 74, 79, 98].

Supervised Fine-Tuning (SFT) was initially proposed to alleviate this issue. To move from image-level grounding to precise pixel-level perception, a common strategy [32, 35, 64, 82] is to let LVLMs emit special tokens that trigger pre-trained segmentation models [65] to produce query-aligned masks. Such 'embedding-as-mask' paradigm has also been explored for detection [81], visual grounding [92], video tracking [5, 84], and for depth estimation [7]. However, their benefits of strong supervision come with a trade-off, whereby SFT can overfit LVLMs to the supervised domain and erode foundation level generalisation [50, 95, 96]. This degradation is often accompanied with weakened chain-of-thought [15], undermining the model's reasoning process.

Instead, **Reinforcement Fine-Tuning (RFT)** do not require the heavy supervision signal [102]. Rather than memorising token-level answers, RFT optimises behaviour via task-specific rewards and constraining updates with KL regularisation [57, 91]. As a result, the LVLM's original capabilities are largely preserved. Thanks to open-sourced foundation models [3, 11, 75, 105] and the critic-free, GPU-friendly design of GRPO [24, 68], RFT has gained growing interest, with a wide range of follow-up works for the post-training [31, 59]. Recent efforts focus on visual grounded reasoning [4, 10, 22, 83, 86, 87, 103], which optimises textual responses and implicitly adjusts bounding boxes to localise the supporting evidence. However, these methods lack explicit object-level learning signal, making them difficult to guarantee fine-grained grounding during reasoning. Our work follows a distinct line of research that directly optimises the policy to generate bounding boxes [52], predict points [29, 89], or handle counting tasks under multi-object scenarios [51]. While previous methods struggle with hard samples when all generated responses fail to identify the correct object, limiting the policy optimisation. In contrast, our approach treats the initial response as an intermediate step and generates a group of follow-up candidates to collaboratively revise it. This group-based revision strategy better handles ambiguous references and enables the model to recover informative signals even in challenging cases.

Reward Shaping [2, 14, 56] is commonly used to mitigate sparse or delayed supervision by providing denser learning feedback. Potential–based shaping [56] formalises this idea and has been widely adopted as a principled way to inject intermediate guidance without changing the target behavior. Recent analyses highlight its practical capabilities [78] in the field of multi-agent system [19, 20] and robotics manipulation [9, 12]. Process Reward Models (PRMs) [42, 69, 88, 101] can be viewed as a form of shaping that delivers step wise feedback in linguistic reasoning tasks [17, 41, 99]. However, transferring such fine grained signals to object grounding is difficult, since intermediate reasoning steps is hard to reliably aligned with concrete image objects. Rather than addressing this step-wise alignment challenge, our consolidation process draws on the core principle of reward shaping. It converts the improvements of the revision group over the initial response into dense feedback that shapes rewards and scales advantages, allowing the model to effectively learn from hard cases.

3. Methodologies

3.1. Preliminary

Let a sample from the dataset be $(x, q, y) \in \mathcal{D}$, where each image $x \in \mathcal{X}$ is paired with a question $q \in \mathcal{Q}$. The corresponding supervision is $y = (\mathbf{b}, \mathbf{p}) \in \mathcal{Y}$, where $\mathbf{b} \in \mathbb{R}^{N_x \times 4}$ represents the bounding boxes of the referenced objects and $\mathbf{p} \in \mathbb{R}^{N_x \times 2}$ provides point coordinates lying inside each object. Here, N_x is the number of annotated objects in image x. In the GRPO setting [68], a policy model $\pi_{\boldsymbol{\theta}}$ parameterised by $\boldsymbol{\theta}$ is optimised using the rollouts collected by a previous (behaviour) policy snapshot $\pi_{\boldsymbol{\theta}_{\texttt{old}}}$, while a frozen reference policy $\pi_{\texttt{ref}}$ provides a per-token forward KL regularisation term. For each training case, a response $o \sim \pi_{\boldsymbol{\theta}_{\texttt{old}}}(\cdot \mid x, q)$ is sampled. Following [50, 51], the response is parsed as $o = (t, \hat{\mathbf{b}}, \hat{\mathbf{p}})$ using a deterministic parser, where t is the generated reasoning text, $\hat{\mathbf{b}} \in \mathbb{R}^{M \times 4}$ and $\hat{\mathbf{p}} \in \mathbb{R}^{M \times 2}$ are the predicted bounding boxes and points, respectively. Here M denotes the number of predicted objects and may differ from N_x. These predicted boxes and points form the object-level grounding outputs that our optimisation aims to refine, identifying the referenced objects and their precise spatial locations. To guide this optimisation, the reward is computed based on the grounding accuracy and the format of the response o. Specifically, an accuracy term $\mathcal{R}_{\texttt{acc}}(o, y)$ measures spatial alignment with the ground truth (e.g., L1 or IoU), while a format term $\mathcal{R}_{\texttt{format}}(o)$ checks whether the response adheres to the expected output structure (e.g., `<think>...</think>` before `<answer>...</answer>`) [10, 29, 50, 51].

3.2. Group Revision and Policy Optimisation

As shown in Fig. 2, our training starts with a sampling phase that generates an initial response, followed by a group of revised results conditioned on it. Next, a consolidation phase computes a shaping signal that quantifies the improvement achieved through the revision. Finally, this signal is used for both reward calculation and advantage scaling.

Response Sampling. We first sample a *single* response from the behavior policy as:

$$(t^{(1)}, \hat{\mathbf{b}}^{(1)}, \hat{\mathbf{p}}^{(1)}) = o^{(1)} \sim \pi_{\boldsymbol{\theta}_{\texttt{old}}}(\cdot \mid x, q), \qquad (1)$$

where $t^{(1)}$ is the reasoning text, and $\hat{\mathbf{b}}^{(1)}, \hat{\mathbf{p}}^{(1)}$ are the predicted bounding boxes and points[1]. This output defines the

[1] If the $o^{(1)}$ format is invalid or does not meet the expected specification, we fall back to the GRPO update procedure as described in [50, 51].

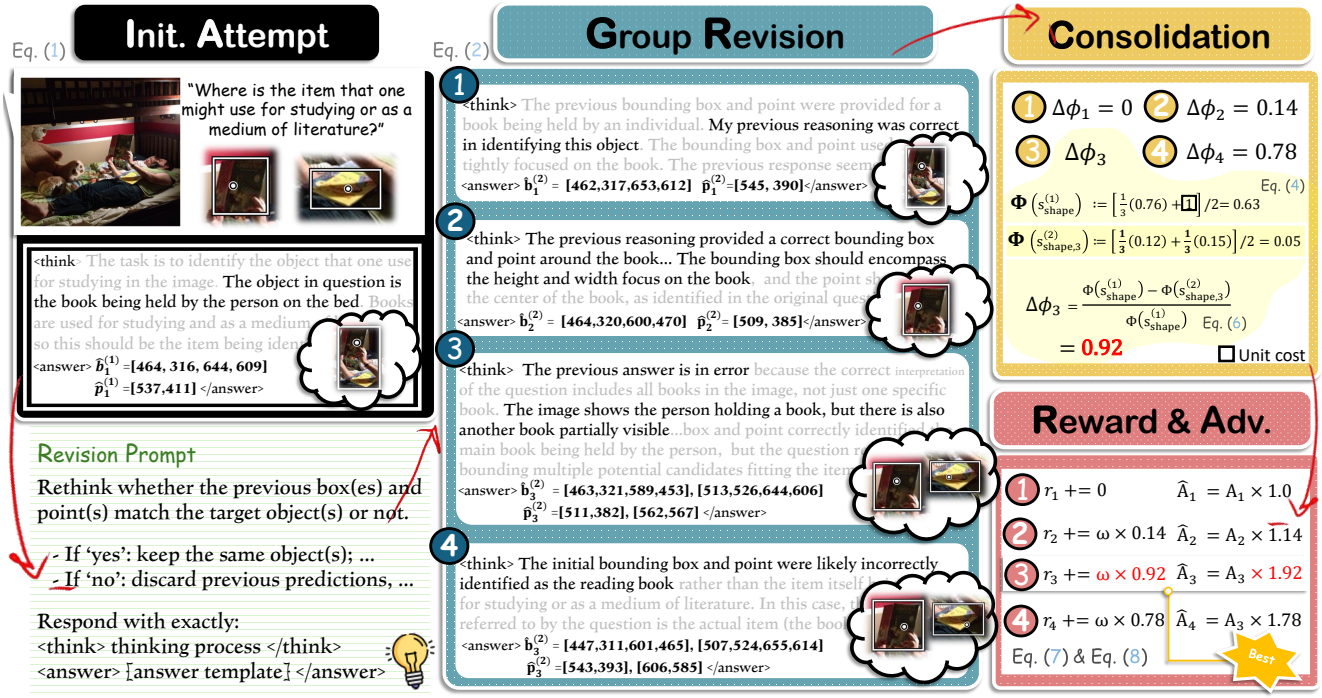

Figure 2. **Illustration of our approach.** We first sample and collect the output from the initial response (Eq. (1)). A revision prompt is appended as a follow-up question to guide the sampling of a group of revised responses (Eq. (2)). We then collect the shaping sets from both results and compute the shaping signal $\Delta\phi_i$ (Eq. (6)) between them. This signal is derived from the alignment cost (Eq. (4)), based on object-wise matching with the ground truth (Eq. (5)). Finally, the signal is used for reward (Eq. (7)) and advantage scaling (Eq. (8)).

initial shaping set $s^{(1)}_{\text{shape}} = \{\hat{\mathbf{b}}^{(1)}, \hat{\mathbf{p}}^{(1)}, y\}$.
We then update the original question into a dialogue-style revised query $q^{(2)} = \mathtt{U}(q, o^{(1)})$ via a fixed revision prompt template, incorporating cues from $t^{(1)}$ and spatial signals $(\hat{\mathbf{b}}^{(1)}, \hat{\mathbf{p}}^{(1)})$. Based on the previous output, a *group* of revision responses is sampled as:

$$o_i^{(2)} \sim \pi_{\theta_{\text{old}}}\left(\cdot \mid x,\, q^{(2)},\, o^{(1)}\right), \quad \text{for } i = 1, \ldots, G. \tag{2}$$

Here, G denotes the group size, and each revision response $o_i^{(2)}$ serves as an alternative grounding hypothesis and potentially resolving ambiguities in challenging scenes. We then construct a per-candidate revision shaping set:

$$s^{(2)}_{\text{shape},i} = \left\{ o_i^{(2)},\, y \;\middle|\; o_i^{(2)} = (t_i^{(2)}, \hat{\mathbf{b}}_i^{(2)}, \hat{\mathbf{p}}_i^{(2)}) \right\}. \tag{3}$$

For convenience, we denote the collected shaping sets uniformly as $s^{(r)}_{\text{shape},i}$, where $r \in \{1, 2\}$ and $i = 1$ when $r = 1$ (the single initial response) or $i \in \{1, \ldots, G\}$ when $r = 2$ (the group of revised outputs). These shaping sets are used solely for computing rewards and advantage post-scaling.

Consolidation Process. We compute the Hungarian matching between the predicted objects $\{(\hat{\mathbf{b}}_m^{(r)}, \hat{\mathbf{p}}_m^{(r)})\}_{m=1}^{M_i^{(r)}}$ and the ground truth $\{(\mathbf{b}_n, \mathbf{p}_n)\}_{n=1}^{N_x}$, where $M_i^{(r)}$ is the number of predictions and N_x is the number of ground truth objects. If $M_i^{(r)} < N_x$, we pad the assignment with $N_x - M_i^{(r)}$ dummy predictions (each incurring a unit cost) to penalise unmatched false negatives. Thus, we obtain the matching set $\mathcal{A}_i^{(r)} \subseteq \{1, \ldots, M_i^{(r)}\} \times \{1, \ldots, N_x\}$. Inspired by potential-based reward shaping [56], we define a potential function $\Phi : s^{(r)}_{\text{shape}} \to \mathbb{R}$ that assigns a scalar to each set, enabling us to quantify the improvement introduced by the revision step. Given the Hungarian matching $\mathcal{A}_i^{(r)}$ for $s^{(r)}_{\text{shape},i}$, the alignment cost can be calculated as:

$$\Phi\left(s^{(r)}_{\text{shape},i}\right) := \frac{1}{|\mathcal{A}_i^{(r)}|} \sum_{(m,n)\in\mathcal{A}_i^{(r)}} e^{(r)}_{m,n}. \tag{4}$$

Here, $e^{(r)}_{m,n}$ denotes the pairwise cost between the object-level results and the ground truth, which is computed as:

$$e^{(r)}_{m,n} = \frac{1}{3}\left[\left(1 - \text{IoU}(\hat{\mathbf{b}}_m^{(r)}, \mathbf{b}_n)\right) + \widetilde{\text{L1}}(\hat{\mathbf{b}}_m^{(r)}, \mathbf{b}_n) + \widetilde{\text{L1}}(\hat{\mathbf{p}}_m^{(r)}, \mathbf{p}_n)\right], \tag{5}$$

where $\widetilde{\text{L1}}$ denotes the L1 distance normalized by the image scale (for both boxes and points). A *lower* pairwise cost $e^{(r)}_{m,n}$ indicates *better* grounding, as the predicted coordinates are closer to the ground truth.
Based on the difference between the alignment costs of the two sets, we derive the shaping signal as:

$$\Delta\phi_i = \max\left(0,\, \frac{\Phi\left(s^{(1)}_{\text{shape}}\right) - \Phi\left(s^{(2)}_{\text{shape},i}\right)}{\Phi\left(s^{(1)}_{\text{shape}}\right)}\right), \tag{6}$$

where $\Delta\phi_i > 0$ means the revision improves upon the initial response and we avoid negative shaping signal in the

optimisation. The denominator $\Phi(s^{(1)}_{\text{shape}})$ provides a per-sample reference scale, so $\Delta\phi_i$ measures the relative improvement with respect to the initial response performance. When the initial is already close to the ground truth and the improvement space is limited (i.e., $\Phi(s^{(1)}_{\text{shape}}) \approx 0$), this scaling prevents the shaping signal from vanishing.

Reward and Advantage. We define the overall reward for each revision group candidate as:

$$r_i = \mathcal{R}_{\texttt{format}}\big(o_i^{(2)}\big) + \mathcal{R}_{\texttt{acc}}\big(o_i^{(2)}, y\big) + \omega\,\Delta\phi_i, \qquad (7)$$

where $\mathcal{R}_{\texttt{format}}$ and $\mathcal{R}_{\texttt{acc}}$ terms following [51] to check the basic performance of $o_i^{(2)}$ for the format and the accuracy. The shaping signal $\Delta\phi_i$ measures the improvement over the initial prediction, with ω controlling its weight.

Following the GRPO optimisation [68], we compute a z-score advantage $A_i = (r_i - \mu)/\sigma$, where μ and σ are the mean and standard deviation computed over the G candidates within the same case. We post-scale this advantage A_i to emphasise samples with larger improvements:

$$\hat{A}_i = (1 + \Delta\phi_i)\, A_i, \qquad (8)$$

where $\Delta\phi_i$ is the relative improvement defined in Eq. (6). We highlight this post-scaling $\hat{A}_i$ serves the different purpose with r_i. The reward r_i determines preference and ranking in GRPO, whereas post-scaling from Eq. (8) adjusts gradient magnitude, highlighting candidates with larger revision gains without altering the objective's sign or form.

Optimisation objective. In the last, we formulate our optimisation function as shown below:

$$\mathcal{J}_{\text{GRPO}}(\theta) = \mathbb{E}\left[\begin{array}{c}(x,q)\sim\mathcal{D},\ o^{(1)}\sim\pi_{\theta_{\texttt{old}}}(\cdot\mid x,q),\\ q^{(2)}=\texttt{U}(q,o^{(1)}),\ \{o_i^{(2)}\}_{i=1}^{G}\sim\pi_{\theta_{\texttt{old}}}(\cdot\mid x,q^{(2)},o^{(1)})\end{array}\right]$$
$$\frac{1}{G}\sum_{i=1}^{G}\min\Big(\ell_i(\boldsymbol{\theta})\,\hat{A}_i,\ \text{clip}(\ell_i(\boldsymbol{\theta}),1-\epsilon,1+\epsilon)\hat{A}_i\Big) - \beta\,\text{KL}\big), \qquad (9)$$

where $\ell_i(\boldsymbol{\theta}) \triangleq \dfrac{\pi_{\boldsymbol{\theta}}(o_i^{(2)}\mid x,q^{(2)})}{\pi_{\theta_{\texttt{old}}}(o_i^{(2)}\mid x,q^{(2)})}$ is the likelihood (importance) ratio between the current and old policy. The ratio clipping with threshold ϵ limits the update induced by $\ell_i(\boldsymbol{\theta})$, preventing excessively large steps. The KL term is $\text{KL}\big(\pi_{\boldsymbol{\theta}}(\cdot\mid x,q^{(2)})\,\|\,\pi_{\texttt{ref}}(\cdot\mid x,q^{(2)})\big)$, which regularises the policy towards a fixed reference with strength controlled by β. The advantage $\hat{A}_i$ (from Eq. (8)) is post-scaled by the shaping signal to improve sample efficiency during training.

3.3. Inference

Given an image–question pair (x, q), we sample a single response $o = (t, \hat{\mathbf{b}}, \hat{\mathbf{p}}) \sim \pi_{\boldsymbol{\theta}}(\cdot \mid x, q)$ with the current policy and parse the predicted objects $\{(\hat{\mathbf{b}}_m, \hat{\mathbf{p}}_m)\}_{m=1}^{M}$, where M is the number of predicted objects. Here, the counting result is reported based on M. Object localisation uses the predicted boxes $\{\hat{\mathbf{b}}_m\}_{m=1}^{M}$, and segmentation is obtained from the box–point pairs $\{(\hat{\mathbf{b}}_m, \hat{\mathbf{p}}_m)\}_{m=1}^{M}$ based on SAM2 [65].

4. Experiment

Training Datasets. We conduct experiments under both single- [50] and multi-object [51] grounding setups. For the ***single-object*** setting, we adopt RefCOCOg [90] (modified following SegZero [50]), which includes 9,000 image–question pairs, each referring to a specific object. All images are resized to 840×840, and the ground truth consists of the one bounding box and two representative points inside the object. For the ***multi-object*** setting, we use the VisionReasoner7K dataset [51], which combines subsets of referring segmentation [25, 45, 90] and reasoning segmentation [85] datasets, resulting in approximately 7,000 samples. To better reflect practical multi-object grounding scenarios, each sample may contain multiple objects, each annotated with a bounding box and a center point.

Evaluation Dataset. We primarily focus on fine-grained grounding tasks, including segmentation and referring expression comprehension (REC), and additionally evaluate zero-shot generalisation to image-level tasks such as counting and visual question answering (VQA). For the ***segmentation*** task, we evaluate on short, direct queries from RefCOCO (g/+) [90] and complex queries from ReasonSeg [35], with ReasonSeg also serving as an out-of-domain benchmark for the ***single*** setup. For the ***REC*** task, we follow standard practice and convert predicted masks on these segmentation datasets [35, 90] into bounding boxes, which are used to assess grounding accuracy. For ***counting***, we evaluate on two benchmarks, CountBench [58] and PixMo-Count [18], by directly counting the number of predicted boxes without any additional counting supervision. We further evaluate our method on ***VQA*** datasets [23, 37, 43, 48, 54, 94] to investigate how object-level Reinforcement learning influences image-level understanding.

Implementation Details. Our method is build on top of Qwen2.5VL-7B [3] as the base LVLM, with SAM2 [65] added for segmentation. The training pipeline adopts the VeRL [71] framework with the vLLM [34] engine, which supports both data and tensor parallelism. Following prior work [50, 51], we use a learning rate of 1e-6 and weight decay of 0.01. The default GRPO group size is 8, the batch size is 64, and the policy is updated every 2 steps. Please refer to Supp. Section A for more implementation details.

Metrics. Following [45, 50], we use generalised Intersection over Union (gIoU) to evaluate pixel-level segmentation on ReasonSeg [35], and cumulative IoU (cIoU) to assess referring segmentation [90]. We also report object-count accuracy and Acc@0.5 for REC, using an IoU threshold of 0.5 for predicted bounding boxes.

4.1. Results across Different Tasks

Segmentation and Counting. In Tab. 1, we compare our method with prior SOTA approaches on both segmentation and counting. For segmentation, we observe con-

Table 1. **Comparison with SoTA on Segmentation and Counting Tasks.** We compare our method with prior SoTA approaches in reasoning segmentation [35] (evaluated with gIoU), referring segmentation [90] (cIoU), and counting [18, 58] (accuracy). $*$ denotes zero-shot performance on the reasoning segmentation task; # indicates re-implemented results based on officially released checkpoints; † marks methods using a consistent checkpoint across all benchmarks. The best results are shown in red, and the second-best are underlined. We highlight these SFT methods generally use larger training sets than RFT methods, please see Supp. Section B for more details.

Method	Segmentation (gIoU & cIoU)							Average	Counting (Acc)			Average
	ReasonSeg		RefCOCO		RefCOCO+		RefCOCOg		Pixmo		Count	
	val	test	testA	testB	testA	testB	test		val	test	test	
LLaVA-OV-7B [38] [arxiv 2024]	-	-	58.1	–	47.1	–	55.6	-	-	-	-	-
LISA-7B [35] [CVPR 2024]	44.4	36.8	79.1	72.3	70.8	58.1	70.6		-	-	-	-
PixelLM-7B [66] [CVPR 2024]	-	-	76.5	68.2	71.7	58.3	70.5	-	-	-	-	-
PerceptionGPT-7B [60] [CVPR 2024]	-	-	78.6	71.7	73.9	61.3	71.7	-	-	-	-	-
SEGLLM [77] [ICLR 2025]	57.2	52.4	81.5	75.4	73.0	62.5	73.6	67.9	-	-	-	-
Read-7B [62] [CVPR 2025]	59.8	56.8	80.2	73.2	73.7	60.4	71.4	67.9	-	-	-	-
Qwen2-VL-7B$^{*\#\dagger}$ [75] [arxiv 2024]	44.5	38.7	58.9	48.0	52.3	41.9	52.1	48.1	29.9	48.0	76.5	51.5
Qwen2.5-VL-7B$^{*\#\dagger}$ [3] [arxiv 2025]	56.9	52.1	77.9	66.5	74.0	55.6	70.9	64.8	63.3	67.9	76.0	69.1
Seg-R1-7B* [89] [arXiv 2025]	58.6	56.7	78.7	67.6	70.9	57.9	71.4	66.0	-	-	-	-
Seg-Zero-7B* [50] [arXiv 2025]	62.6	57.5	80.3	72.2$^{\#}$	76.2	62.3$^{\#}$	72.6	69.1	-	-	-	-
VisionReasoner-7B† [51] [arXiv 2025]	66.3	63.6	77.4$^{\#}$	67.6$^{\#}$	71.1$^{\#}$	55.8$^{\#}$	68.3$^{\#}$	67.2	70.1	69.5	87.6	75.7
Ours (single-object)*	66.99	61.11	80.79	73.16	76.72	62.92	74.26	70.85	-	-	-	-
Ours (multi-object)†	67.48	66.73	78.04	69.53	73.30	59.34	71.08	69.36	75.89	72.97	91.04	79.97

Table 2. **Comparison with SoTA methods on the REC task.** We compare with SoTA methods on ReasonG (boxes converted from reasoning segmentation [35]) and referring grounding (RefCOCO (+/g) [90]). # denotes re-implementations using official checkpoints; † denotes a single checkpoint across all benchmarks. The best results are shown in red, and the second-best are underlined.

Method	Referring Expression Comprehension (Acc@0.5)										Average
	ReasonG		RefCOCO			RefCOCO+			RefCOCOg		
	val	test	val	testA	testB	val	testA	testB	val	test	
PerceptionGPT-7B [60] [CVPR 2024]	–	–	88.6	92.5	84.6	82.1	88.6	74.2	84.1	85.2	–
VistaLLM-7B [61] [ECCV 2024]	–	–	88.1	91.5	83.0	82.9	89.8	74.8	83.6	84.4	–
Elysium-7B [73] [ECCV 2024]	–	–	89.1	92.1	85.0	82.9	88.9	75.6	82.9	83.6	–
Groma-7B [53] [ECCV 2024]	–	–	89.5	92.1	86.3	83.9	88.9	78.1	86.3	87.0	–
Qwen2-VL-7B$^{*\#\dagger}$ [75] [arxiv 2024]	54.6	46.9	80.8	83.9	58.9	72.5	76.5	54.5	77.3	78.2	68.4
Qwen2.5-VL-7B$^{*\#\dagger}$ [3] [arxiv 2025]	68.9	59.8	88.8	91.7	81.4	82.3	88.2	69.2	84.7	85.7	80.1
SegZero-7B$^{*\#}$ [50] [arxiv 2025]	69.3	64.6	89.3	91.5	81.9	82.0	87.6	74.7	86.1	86.3	81.3
VisionReasoner-7B† [51] [arxiv 2025]	80.1$^{\#}$	78.5$^{\#}$	88.6	90.6	84.7$^{\#}$	83.6	87.9	80.2$^{\#}$	86.1	87.5	84.8
Ours (single-object)	73.98	66.41	90.72	92.36	86.67	84.49	89.28	74.26	87.64	87.97	83.38
Ours (multi-object)†	83.67	81.20	89.49	91.55	85.05	84.37	88.33	77.60	88.44	88.32	85.80

Table 3. **General VQA.** Comparison on diverse VQA benchmarks for general image understanding. Best results are shown in red.

Model	SeedBenchV2+ [37]	ChartQA [54]	OCRBench [48]
	Acc.	Acc.	Num.
Qwen2.5VL-7B [3]	70.4	83.6	849
Ours (single)	70.75	84.03	853
Ours (multi)	70.95	84.96	861

Model	POPE [43]	MMMU-Pro [94]		MME [23]	
		Vis	Std	Cog.	Percept.
Qwen2.5VL-7B [3]	87.1	32.5	36.4	619.0	1691.9
Ours (single)	88.24	33.12	37.11	627.14	1698.11
Ours (multi)	88.21	33.70	37.75	630.00	1708.01

sistent gains over other RFT-based methods [50, 51, 89]. For example, on ReasonSeg [35] (test), our single-object setup achieves 61.11 gIoU, surpassing Seg-R1 [89] by 7.78 points. For counting, using the consistent checkpoint in multi-object setting, our method attains an average accuracy of 79.97% across two datasets [18, 58], and we observe a 5.64 % improvement over VisionReasoner [51]. Benefiting from the group-revision paradigm, these results indicate more accurate object grounding and localization (both boxes and points) across diverse and challenging scenarios.

Referring Expression Comprehension. As shown in Tab. 2, our model (multi) achieves the best overall Acc@0.5 of 85.80%, surpassing the previous SOTA VisionReasoner [51] by 1.0 points. Although our method shows lower performance on RefCOCO+ (testB) than VisionReasoner, this is largely due to its fewer false-positive boxes: VisionReasoner produces many extra boxes, which inflate Acc@0.5 but are consistent with its lower segmentation quality (shown in Tab. 1). Compared with Seg-Zero [50] under the single-object setting, our method yields notable improvements of 4.58% and 1.81% on ReasonG (val and test, boxes converted from ReasonSeg [35]). These results suggest the benefit of our group-revision optimisation paradigm for improving visually grounded bounding box localisation.

General VQA. In Tab. 3, we use the `llms-eval` [97] toolkit to assess performance across diverse VQA bench-

Table 4. **Ablation study of our approach** on both single-object and multi-object setups. We apply our method on ReasonSeg [35] and RefCOCO+ [90] for the segmentation task, RefCOCOg [90] for the REC task, and PixMoCount [18] for counting (multi-object only). The w/ revision refers to Eq. (2), and w/ consolidation refers to shaping signal in both Eq. (7) and (8). The best results are shown in red.

Ablation Study	Single-Object						Multi-Object							
	Segmentation				REC		Segmentation				REC		Counting	
	ReasonSeg		RefCOCOg		RefCOCOg		ReasonSeg		RefCOCOg		RefCOCOg		Pixmo	
	val	test	val	testA	val	testA	val	test	val	testA	val	testA	val	test
baseline	62.54	58.67	70.84	72.17	85.92	86.67	65.37	64.23	66.87	68.92	87.26	87.20	70.84	70.53
w/ revision	64.97	60.24	70.92	73.80	86.79	87.03	66.54	65.91	69.92	70.04	88.13	88.54	73.20	71.94
w/ consolidation	66.99	61.11	73.58	74.26	87.64	87.97	67.48	66.73	70.67	71.08	88.32	88.44	75.89	72.97

Table 5. **Ablation of Consolidation Weight.** We vary the parameter ω from Eq. (7) under the single-object setting and assess its impact on segmentation [35, 90] and REC [90] tasks.

weight (ω)	Segmentation				REC	
	ReasonSeg		RefCOCOg		RefCOCOg	
	val	test	val	testA	val	testA
3	64.36	59.67	72.86	73.63	87.72	87.89
5	66.99	61.11	73.58	74.26	87.64	87.97
7	65.84	62.07	72.73	73.92	87.03	87.14

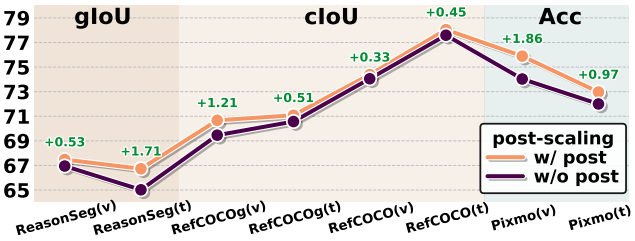

Figure 3. **Ablation of Post Scaling**. We evaluate our method with the effectiveness of advantage post-scaling from Eq. (8) in the segmentation [35, 90] and counting tasks [18] in single-object setting.

marks. Our method (multi) shows consistent gains over [3], achieving +0.55% on SeedBenchV2+ [37] and +1.25% (average) on MMU-pro [93]. These results suggest that object-level grounding improves instance-level localisation and benefits overall image-level understanding.

4.2. Ablation Studies

Ablation in our main contribution. As shown in Tab. 4, both revision sampling and consolidation with reward shaping provide consistent gains in single and multi setups. Training with the revision group steadily improves over directly generated answers (as in GRPO). In the single-object setting, performance on ReasonSeg (val) [35] improves from 62.54% to 64.97%, and on RefCOCOg (val) [90] from 70.84% to 70.92%. Consolidation yields larger boosts by up-weighting higher-reward candidates and amplifying gradients, further increasing these results to 66.99% and 73.84%. The effect is most pronounced on counting: PixMoCount (val) [18] rises from 70.84% to 73.20% with revision, and to 75.89% with consolidation. Overall, revision sampling introduces diverse hypotheses and recovers learning signals, while consolidation effectively amplifies these benefits, leading to robust performance gains.

Table 6. **Ablation of Consolidation Components.** We assess the effect of removing point or box shaping signals (from Eq. (5)) on segmentation [35, 90] and REC [90] tasks.

Variant	Segmentation				REC	
	ReasonSeg		RefCOCOg		RefCOCOg	
	val	test	val	testA	val	testA
w/ both	66.99	61.11	73.58	74.26	87.64	87.97
w/o box	65.32	60.28	71.06	73.48	86.04	86.58
w/o point	65.90	59.97	72.64	73.52	87.59	87.76

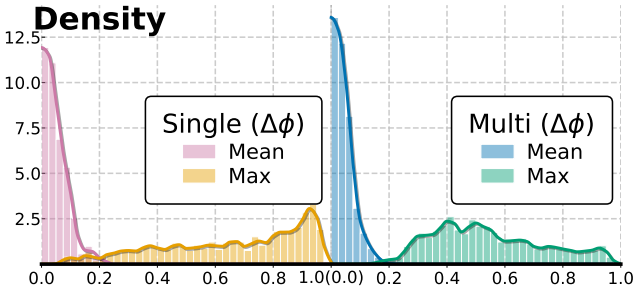

Figure 4. **The $\Delta\phi$ probability density function** for both single- and multi-object setups, reported with groupwise mean and max measurements. Higher density indicates a larger proportion of training samples attaining the corresponding $\Delta\phi$ level.

Ablation on reward weight (ω). In Tab. 5, we study the effect of the shaping weight in the reward on segmentation [35] and REC [90] under the single setup. We observe that $\omega = 3$ and 7 yields slightly better results on specific splits, whereas $\omega = 5$ achieves the best overall results.

Ablation on advantage post-scaling. We evaluate the impact of advantage post-scaling from Eq. (8) in Fig. 3. Consistent gains are observed on all four datasets for both validation and test splits, including improvements of 0.53% and 1.71% points on ReasonSeg [35], and 1.86% and 0.97% points on PixMoCount [18]. These results indicate that scaling strengthens gradient updates during consolidation.

Consolidation signal distribution. Fig. 4 shows the probability density function (PDF) of $\Delta\phi$ from Eq. (6) for both single and multi setups. This PDF illustrates how consolidation gains contribute to the reward term and to advantage scaling. In the single-object setting, the group-wise mean is concentrated around 0-0.2, indicating mild but consistent improvements per sample, while the max exhibits a heavy right tail with most mass between 0.8 and 1.0. This pattern suggests that strong revision candidates do exist and can

Table 7. **Hallucination cases** on the ReasonSeg [35] val. and test splits (with 995 cases in total). The evaluation is conducted on CoT thinking process using an `LLM-as-a-Judge` protocol with GPT-5. More details are provided in the Supp. Section C.

Method	Hallucination cases (#)		
	Off Topic	Mismatch	Vague Claim
SegZero-7B [50]	37	231	52
VisionReasoner [51]	46	194	82
Ours (single)	22	187	35
Ours (multi)	24	142	48

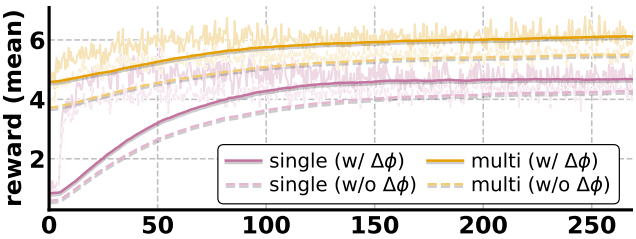

Figure 5. **Reward curves** over training steps for both single- and multi-object setups. Each line shows the mean reward of the revision group in condition of with and without the $\Delta\phi$ term.

be effectively up-weighted, while most cases remain stable. Crucially, the distribution indicates that initial responses are generally of competitive quality and are not intentionally degraded to inflate $\Delta\phi$, reducing the risk of ***reward hacking***. Together, these observations support the stability and integrity of our group-revision optimisation paradigm.

Reasoning Process Evaluation. As shown in Tab. 7, we assess CoT reasoning hallucinations based on GPT-5. We consider three types: *off-topic* (reasoning does not follow the query), *attribute mismatch* (the description does not correctly describe the object inside the bounding box), and *vague claim* (the description is overly generic and not specific to the object). Our method (multi) produces fewer hallucinations than VisionReasoner [51], including -52 cases of attribute mismatch and -22 cases of vague claims. While the single-object setup reduces vague claims, it causes more mismatches, whereas multi-object revision offers more consistent grounding in complex scenes. The fewer hallucination cases in our methods show that optimising on hard cases helps the model produce more accurate CoT.

4.3. Visualisation

Reward Curves. Fig. 5 presents the reward trajectories for both single- and multi-object setups, comparing our method against GRPO (without the revision process). The group revision responses consistently achieves higher rewards, suggesting that revision gains (especially from hard samples) are effectively transformed into stronger learning signals.

Qualitative Results. In Fig. 6, we compare our method with Qwen2.5VL-7B [3] on both the reasoning segmentation [35] and counting [58] benchmarks. Our approach shows consistently better visual performance. For example, in the case of the query '`Something that controls the speed and direction of the boat`', our model produces more coherent reasoning (e.g., correctly identifying the oars) and delivers more accurate spatial grounding.

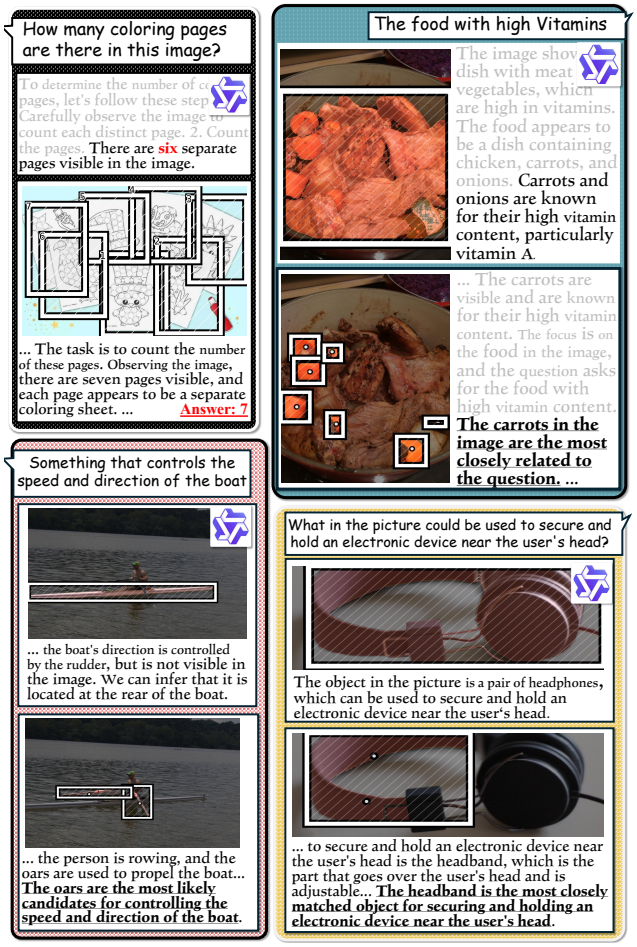

Figure 6. **Qualitative comparisons** on the CountingBench [58] and ReasoningSeg [35] datasets. For each example, we present the outputs from Qwen2.5VL-7B [3] (top row) and our method (bottom), including both CoT reasoning and spatial grounding.

5. Conclusion

In this paper, we introduce a group revision paradigm designed to recover learning signals from hard cases that are overlooked by GRPO. Our approach begins by sampling an initial response and generating a group of revised results conditioned on it. We then introduce a consolidation process that quantifies the improvement of each revised output, yielding a shaping signal used for both reward calculation and advantage scaling. This signal captures the specific improvements introduced by the revision, providing the policy with concrete guidance on which changes led to the corrected outcome. Experiments show that our method consistently improves object-level grounding over previous approaches. These results highlight its effectiveness as a more reliable optimisation paradigm for LVLMs grounding.

References

[1] Jean-Baptiste Alayrac, Jeff Donahue, Pauline Luc, Antoine Miech, Iain Barr, Yana Hasson, Karel Lenc, Arthur Mensch, Katherine Millican, Malcolm Reynolds, et al. Flamingo: a visual language model for few-shot learning. *Advances in neural information processing systems*, 35: 23716–23736, 2022. 2

[2] Marcin Andrychowicz, Filip Wolski, Alex Ray, Jonas Schneider, Rachel Fong, Peter Welinder, Bob McGrew, Josh Tobin, OpenAI Pieter Abbeel, and Wojciech Zaremba. Hindsight experience replay. *Advances in neural information processing systems*, 30, 2017. 3

[3] Shuai Bai, Keqin Chen, Xuejing Liu, Jialin Wang, Wenbin Ge, Sibo Song, Kai Dang, Peng Wang, Shijie Wang, Jun Tang, et al. Qwen2. 5-vl technical report. *arXiv preprint arXiv:2502.13923*, 2025. 1, 2, 3, 5, 6, 7, 8

[4] Sule Bai, Mingxing Li, Yong Liu, Jing Tang, Haoji Zhang, Lei Sun, Xiangxiang Chu, and Yansong Tang. Univg-r1: Reasoning guided universal visual grounding with reinforcement learning. *arXiv preprint arXiv:2505.14231*, 2025. 3

[5] Zechen Bai, Tong He, Haiyang Mei, et al. One token to seg them all: Language-instructed reasoning segmentation in videos. In *NeurIPS*, 2024. 3

[6] Zechen Bai, Pichao Wang, Tianjun Xiao, Tong He, Zongbo Han, Zheng Zhang, and Mike Zheng Shou. Hallucination of multimodal large language models: A survey. *arXiv preprint arXiv:2404.18930*, 2024. 3

[7] Mohammad Bigverdi, Amanpreet Singh, et al. Perception tokens enhance visual reasoning in multimodal language models. In *CVPR*, 2025. 3

[8] Ali Furkan Biten, Lluís Gómez, and Dimosthenis Karatzas. Let there be a clock on the beach: Reducing object hallucination in image captioning. In *Proceedings of the IEEE/CVF Winter Conference on Applications of Computer Vision*, pages 1381–1390, 2022. 2

[9] Alberto Camacho, Jacob Varley, Andy Zeng, Deepali Jain, Atil Iscen, and Dmitry Kalashnikov. Reward machines for vision-based robotic manipulation. In *2021 IEEE International Conference on Robotics and Automation (ICRA)*, pages 14284–14290. IEEE, 2021. 3

[10] Meng Cao, Haoze Zhao, Can Zhang, Xiaojun Chang, Ian Reid, and Xiaodan Liang. Ground-r1: Incentivizing grounded visual reasoning via reinforcement learning. *arXiv preprint arXiv:2505.20272*, 2025. 3

[11] Xiaokang Chen, Zhiyu Wu, Xingchao Liu, Zizheng Pan, Wen Liu, Zhenda Xie, Xingkai Yu, and Chong Ruan. Janus-pro: Unified multimodal understanding and generation with data and model scaling. *arXiv preprint arXiv:2501.17811*, 2025. 1, 3

[12] Yifei Chen, Lambert Schomaker, and Francisco Cruz. Boosting reinforcement learning algorithms in continuous robotic reaching tasks using adaptive potential functions. In *Australasian Joint Conference on Artificial Intelligence*, pages 52–64. Springer, 2024. 3

[13] Zhe Chen, Weiyun Wang, Yue Cao, Yangzhou Liu, Zhangwei Gao, Erfei Cui, Jinguo Zhu, Shenglong Ye, Hao Tian, Zhaoyang Liu, et al. Expanding performance boundaries of open-source multimodal models with model, data, and test-time scaling. *arXiv preprint arXiv:2412.05271*, 2024. 2

[14] Paul F Christiano, Jan Leike, Tom Brown, Miljan Martic, Shane Legg, and Dario Amodei. Deep reinforcement learning from human preferences. *Advances in neural information processing systems*, 30, 2017. 2, 3

[15] Hyung Won Chung, Le Hou, Shayne Longpre, Barret Zoph, Yi Tay, William Fedus, Yunxuan Li, Xuezhi Wang, Mostafa Dehghani, Siddhartha Brahma, et al. Scaling instruction-finetuned language models. *Journal of Machine Learning Research*, 25(70):1–53, 2024. 3

[16] Gheorghe Comanici, Eric Bieber, Mike Schaekermann, Ice Pasupat, Noveen Sachdeva, Inderjit Dhillon, Marcel Blistein, Ori Ram, Dan Zhang, Evan Rosen, et al. Gemini 2.5: Pushing the frontier with advanced reasoning, multimodality, long context, and next generation agentic capabilities. *arXiv preprint arXiv:2507.06261*, 2025. 1

[17] Ning Dai, Zheng Wu, Renjie Zheng, Ziyun Wei, Wenlei Shi, Xing Jin, Guanlin Liu, Chen Dun, Liang Huang, and Lin Yan. Process supervision-guided policy optimization for code generation. *arXiv preprint arXiv:2410.17621*, 2024. 2, 3

[18] Matt Deitke, Christopher Clark, Sangho Lee, Rohun Tripathi, Yue Yang, Jae Sung Park, Mohammadreza Salehi, Niklas Muennighoff, Kyle Lo, Luca Soldaini, et al. Molmo and pixmo: Open weights and open data for state-of-the-art vision-language models. In *Proceedings of the Computer Vision and Pattern Recognition Conference*, pages 91–104, 2025. 2, 5, 6, 7

[19] Sam Devlin, Logan Yliniemi, Daniel Kudenko, and Kagan Tumer. Potential-based difference rewards for multiagent reinforcement learning. In *Proceedings of the 2014 international conference on Autonomous agents and multi-agent systems*, pages 165–172, 2014. 3

[20] Sam Michael Devlin and Daniel Kudenko. Dynamic potential-based reward shaping. In *11th International Conference on Autonomous Agents and Multiagent Systems (AAMAS 2012)*, pages 433–440. IFAAMAS, 2012. 3

[21] Danny Driess, Fei Xia, Mehdi SM Sajjadi, Corey Lynch, Aakanksha Chowdhery, Brian Ichter, Ayzaan Wahid, Jonathan Tompson, Quan Vuong, Tianhe Yu, et al. Palm-e: An embodied multimodal language model. *arXiv preprint arXiv:2303.03378*, 2023. 2

[22] Kaituo Feng, Kaixiong Gong, Bohao Li, Zonghao Guo, Yibing Wang, Tianshuo Peng, Junfei Wu, Xiaoying Zhang, Benyou Wang, and Xiangyu Yue. Video-r1: Reinforcing video reasoning in mllms. *arXiv preprint arXiv:2503.21776*, 2025. 3

[23] Chaoyou Fu, Peixian Chen, Yunhang Shen, Yulei Qin, Mengdan Zhang, Xu Lin, Jinrui Yang, Xiawu Zheng, Ke Li, Xing Sun, et al. Mme: A comprehensive evaluation benchmark for multimodal large language models. In *The Thirty-ninth Annual Conference on Neural Information Processing Systems Datasets and Benchmarks Track*, 2025. 5, 6

[24] Dong Guo, Zichen Liu, Weize Zhang, Yuxuan Zhou, Xiaozhi Wang, et al. Deepseek-r1: Incentivizing reasoning ca-

pability in llms via reinforcement learning. *arXiv preprint arXiv:2501.12948*, 2025. Uses GRPO for reasoning RL. 3

[25] Agrim Gupta, Piotr Dollar, and Ross Girshick. Lvis: A dataset for large vocabulary instance segmentation. In *Proceedings of the IEEE/CVF conference on computer vision and pattern recognition*, pages 5356–5364, 2019. 5

[26] Bo He, Hengduo Li, Young Kyun Jang, Menglin Jia, Xuefei Cao, Ashish Shah, Abhinav Shrivastava, and Ser-Nam Lim. Ma-lmm: Memory-augmented large multimodal model for long-term video understanding. In *Proceedings of the IEEE/CVF Conference on Computer Vision and Pattern Recognition*, pages 13504–13514, 2024. 2

[27] Cheng-Yu Hsieh, Jieyu Zhang, Zixian Ma, Aniruddha Kembhavi, and Ranjay Krishna. Sugarcrepe: Fixing hackable benchmarks for vision-language compositionality. *Advances in neural information processing systems*, 36: 31096–31116, 2023. 1

[28] Haifeng Huang, Xinyi Chen, Yilun Chen, Hao Li, Xiaoshen Han, Zehan Wang, Tai Wang, Jiangmiao Pang, and Zhou Zhao. Roboground: Robotic manipulation with grounded vision-language priors. In *Proceedings of the Computer Vision and Pattern Recognition Conference*, pages 22540–22550, 2025. 1, 3

[29] Jiaqi Huang, Zunnan Xu, Jun Zhou, Ting Liu, Yicheng Xiao, Mingwen Ou, Bowen Ji, Xiu Li, and Kehong Yuan. Sam-r1: Leveraging sam for reward feedback in multimodal segmentation via reinforcement learning. *arXiv preprint arXiv:2505.22596*, 2025. 1, 3

[30] Ziwei Ji, Nayeon Lee, Rita Frieske, Tiezheng Yu, Dan Su, Yan Xu, Etsuko Ishii, Ye Jin Bang, Andrea Madotto, and Pascale Fung. Survey of hallucination in natural language generation. *ACM computing surveys*, 55(12):1–38, 2023. 1, 2

[31] Qing Jiang, Xingyu Chen, Zhaoyang Zeng, Junzhi Yu, and Lei Zhang. Rex-thinker: Grounded object referring via chain-of-thought reasoning. *arXiv preprint arXiv:2506.04034*, 2025. 3

[32] Alexander Kirillov, Eric Mintun, Nikhila Ravi, Hanzi Mao, Chloe Rolland, Laura Gustafson, Tete Xiao, Spencer Whitehead, Alexander C Berg, Wan-Yen Lo, et al. Segment anything. In *Proceedings of the IEEE/CVF international conference on computer vision*, pages 4015–4026, 2023. 3

[33] Christoph F Kurz, Tatiana Merzhevich, Bjoern M Eskofier, Jakob Nikolas Kather, and Benjamin Gmeiner. Benchmarking vision-language models for diagnostics in emergency and critical care settings. *npj Digital Medicine*, 8(1):423, 2025. 1

[34] Woosuk Kwon, Zhuohan Li, Siyuan Zhuang, Ying Sheng, Lianmin Zheng, Cody Hao Yu, Joseph E. Gonzalez, Hao Zhang, and Ion Stoica. Efficient memory management for large language model serving with pagedattention. In *Proceedings of the ACM SIGOPS 29th Symposium on Operating Systems Principles*, 2023. 5

[35] Xin Lai, Zhuotao Tian, Yukang Chen, Yanwei Li, Yuhui Yuan, Shu Liu, and Jiaya Jia. Lisa: Reasoning segmentation via large language model. In *Proceedings of the IEEE/CVF Conference on Computer Vision and Pattern Recognition*, pages 9579–9589, 2024. 1, 2, 3, 5, 6, 7, 8

[36] Sicong Leng, Hang Zhang, Guanzheng Chen, Xin Li, Shijian Lu, Chunyan Miao, and Lidong Bing. Mitigating object hallucinations in large vision-language models through visual contrastive decoding. In *Proceedings of the IEEE/CVF Conference on Computer Vision and Pattern Recognition*, pages 13872–13882, 2024. 1, 2

[37] Bohao Li, Yuying Ge, Yi Chen, Yixiao Ge, Ruimao Zhang, and Ying Shan. Seed-bench-2-plus: Benchmarking multimodal large language models with text-rich visual comprehension. *arXiv preprint arXiv:2404.16790*, 2024. 5, 6, 7

[38] Bo Li, Yuanhan Zhang, Dong Guo, Renrui Zhang, Feng Li, Hao Zhang, Kaichen Zhang, Peiyuan Zhang, Yanwei Li, Ziwei Liu, et al. Llava-onevision: Easy visual task transfer. *arXiv preprint arXiv:2408.03326*, 2024. 6

[39] Junnan Li, Dongxu Li, Caiming Xiong, and Steven Hoi. Blip: Bootstrapping language-image pre-training for unified vision-language understanding and generation. In *International conference on machine learning*, pages 12888–12900. PMLR, 2022. 1

[40] Junnan Li, Dongxu Li, Silvio Savarese, and Steven Hoi. Blip-2: Bootstrapping language-image pre-training with frozen image encoders and large language models. In *International conference on machine learning*, pages 19730–19742. PMLR, 2023. 2

[41] Qingyao Li, Xinyi Dai, Xiangyang Li, Weinan Zhang, Yasheng Wang, Ruiming Tang, and Yong Yu. Codeprm: Execution feedback-enhanced process reward model for code generation. In *Findings of the Association for Computational Linguistics: ACL 2025*, pages 8169–8182, 2025. 2, 3

[42] Wendi Li and Yixuan Li. Process reward model with q-value rankings. *arXiv preprint arXiv:2410.11287*, 2024. 3

[43] Yifan Li, Yifan Du, Kun Zhou, Jinpeng Wang, Wayne Xin Zhao, and Ji-Rong Wen. Evaluating object hallucination in large vision-language models. *arXiv preprint arXiv:2305.10355*, 2023. 5, 6

[44] Hunter Lightman, Vineet Kosaraju, Yura Burda, Harri Edwards, Bowen Baker, Teddy Lee, Jan Leike, John Schulman, Ilya Sutskever, and Karl Cobbe. Let's verify step by step. *arXiv preprint arXiv:2305.20050*, 2023. 2

[45] Chang Liu, Henghui Ding, and Xudong Jiang. Gres: Generalized referring expression segmentation. In *Proceedings of the IEEE/CVF conference on computer vision and pattern recognition*, pages 23592–23601, 2023. 5

[46] Haotian Liu, Chunyuan Li, Qingyang Wu, and Yong Jae Lee. Visual instruction tuning. *Advances in neural information processing systems*, 36:34892–34916, 2023. 1, 2

[47] Hanchao Liu, Wenyuan Xue, Yifei Chen, Dapeng Chen, Xiutian Zhao, Ke Wang, Liping Hou, Rongjun Li, and Wei Peng. A survey on hallucination in large vision-language models. *arXiv preprint arXiv:2402.00253*, 2024. 1, 2

[48] Yuliang Liu, Zhang Li, Mingxin Huang, Biao Yang, Wenwen Yu, Chunyuan Li, Xu-Cheng Yin, Cheng-Lin Liu, Lianwen Jin, and Xiang Bai. Ocrbench: on the hidden mystery of ocr in large multimodal models. *Science China Information Sciences*, 67(12):220102, 2024. 5, 6

[49] Yuyuan Liu, Yuanhong Chen, Chong Wang, Junlin Han, Junde Wu, Can Peng, Jingkun Chen, Yu Tian, and Gustavo Carneiro. Auralsam2: Enabling sam2 hear through pyramid audio-visual feature prompting. *arXiv preprint arXiv:2506.01015*, 2025. 3

[50] Yuqi Liu, Bohao Peng, Zhisheng Zhong, Zihao Yue, Fanbin Lu, Bei Yu, and Jiaya Jia. Seg-zero: Reasoning-chain guided segmentation via cognitive reinforcement. *arXiv preprint arXiv:2503.06520*, 2025. 1, 2, 3, 5, 6, 8

[51] Yuqi Liu, Tianyuan Qu, Zhisheng Zhong, Bohao Peng, Shu Liu, Bei Yu, and Jiaya Jia. Visionreasoner: Unified visual perception and reasoning via reinforcement learning. *arXiv preprint arXiv:2505.12081*, 2025. 1, 3, 5, 6, 8

[52] Ziyu Liu, Zeyi Sun, Yuhang Zang, Xiaoyi Dong, Yuhang Cao, Haodong Duan, Dahua Lin, and Jiaqi Wang. Visual-rft: Visual reinforcement fine-tuning. *arXiv preprint arXiv:2503.01785*, 2025. 1, 2, 3

[53] Chuofan Ma, Yi Jiang, Jiannan Wu, Zehuan Yuan, and Xiaojuan Qi. Groma: Localized visual tokenization for grounding multimodal large language models. In *European Conference on Computer Vision*, pages 417–435. Springer, 2024. 6

[54] Ahmed Masry, Xuan Long Do, Jia Qing Tan, Shafiq Joty, and Enamul Hoque. Chartqa: A benchmark for question answering about charts with visual and logical reasoning. In *Findings of the association for computational linguistics: ACL 2022*, pages 2263–2279, 2022. 5, 6

[55] Youssef Mroueh, Nicolas Dupuis, Brian Belgodere, Apoorva Nitsure, Mattia Rigotti, Kristjan Greenewald, Jiri Navratil, Jerret Ross, and Jesus Rios. Revisiting group relative policy optimization: Insights into on-policy and off-policy training. *arXiv preprint arXiv:2505.22257*, 2025. 2

[56] Andrew Y Ng, Daishi Harada, and Stuart Russell. Policy invariance under reward transformations: Theory and application to reward shaping. In *Icml*, pages 278–287. Citeseer, 1999. 2, 3, 4

[57] Long Ouyang, Jeff Wu, Xu Jiang, Diogo Almeida, Carroll Wainwright, Pamela Mishkin, Chong Zhang, Sandhini Agarwal, Katarina Slama, Alex Ray, et al. Training language models to follow instructions with human feedback. In *Advances in Neural Information Processing Systems (NeurIPS)*, 2022. 3

[58] Roni Paiss, Ariel Ephrat, Omer Tov, Shiran Zada, Inbar Mosseri, Michal Irani, and Tali Dekel. Teaching clip to count to ten. In *Proceedings of the IEEE/CVF International Conference on Computer Vision*, pages 3170–3180, 2023. 1, 2, 5, 6, 8

[59] Jiazhen Pan, Che Liu, Junde Wu, Fenglin Liu, Jiayuan Zhu, Hongwei Bran Li, Chen Chen, Cheng Ouyang, and Daniel Rueckert. Medvlm-r1: Incentivizing medical reasoning capability of vision-language models via reinforcement learning. *arXiv preprint arXiv:2502.19634*, 2025. 3

[60] Renjie Pi, Lewei Yao, Jiahui Gao, Jipeng Zhang, and Tong Zhang. Perceptiongpt: Effectively fusing visual perception into llm. In *Proceedings of the IEEE/CVF conference on computer vision and pattern recognition*, pages 27124–27133, 2024. 6

[61] Shraman Pramanick, Guangxing Han, Rui Hou, Sayan Nag, Ser-Nam Lim, Nicolas Ballas, Qifan Wang, Rama Chellappa, and Amjad Almahairi. Jack of all tasks master of many: Designing general-purpose coarse-to-fine vision-language model. In *Proceedings of the IEEE/CVF Conference on Computer Vision and Pattern Recognition*, pages 14076–14088, 2024. 6

[62] Rui Qian, Xin Yin, and Dejing Dou. Reasoning to attend: Try to understand how< seg> token works. In *Proceedings of the IEEE/CVF Conference on Computer Vision and Pattern Recognition*, 2025. 6

[63] Yanyuan Qiao, Haodong Hong, Wenqi Lyu, Dong An, Siqi Zhang, Yutong Xie, Xinyu Wang, and Qi Wu. Navbench: Probing multimodal large language models for embodied navigation. *arXiv preprint arXiv:2506.01031*, 2025. 1

[64] Hanoona Rasheed, Muhammad Maaz, Sahal Shaji, Abdelrahman Shaker, Salman Khan, Hisham Cholakkal, Rao M Anwer, Eric Xing, Ming-Hsuan Yang, and Fahad S Khan. Glamm: Pixel grounding large multimodal model. In *Proceedings of the IEEE/CVF Conference on Computer Vision and Pattern Recognition*, pages 13009–13018, 2024. 3

[65] Nikhila Ravi, Valentin Gabeur, Yuan-Ting Hu, Ronghang Hu, Chaitanya Ryali, Tengyu Ma, Haitham Khedr, Roman Rädle, Chloe Rolland, Laura Gustafson, Eric Mintun, Junting Pan, Kalyan Vasudev Alwala, Nicolas Carion, Chao-Yuan Wu, Ross Girshick, Piotr Dollár, and Christoph Feichtenhofer. Sam 2: Segment anything in images and videos. *arXiv preprint arXiv:2408.00714*, 2024. 1, 3, 5

[66] Zhongwei Ren, Zhicheng Huang, Yunchao Wei, Yao Zhao, Dongmei Fu, Jiashi Feng, and Xiaojie Jin. Pixellm: Pixel reasoning with large multimodal model. In *Proceedings of the IEEE/CVF Conference on Computer Vision and Pattern Recognition*, pages 26374–26383, 2024. 6

[67] Anna Rohrbach, Lisa Anne Hendricks, Kaylee Burns, Trevor Darrell, and Kate Saenko. Object hallucination in image captioning. *arXiv preprint arXiv:1809.02156*, 2018. 1, 2

[68] Zhihong Shao, Zihan Zhang, Xinyu Huang, Yushi Yang, Minghui Qiu, and Wayne Xin Zhao. Deepseekmath: Pushing the limits of mathematical reasoning in open language models. *arXiv preprint arXiv:2402.03300*, 2024. Introduces Group-Relative Policy Optimization (GRPO). 1, 3, 5

[69] Shuaijie She, Junxiao Liu, Yifeng Liu, Jiajun Chen, Xin Huang, and Shujian Huang. R-prm: Reasoning-driven process reward modeling. *arXiv preprint arXiv:2503.21295*, 2025. 3

[70] Haozhan Shen, Peng Liu, Jingcheng Li, Chunxin Fang, Yibo Ma, Jiajia Liao, Qiaoli Shen, Zilun Zhang, Kangjia Zhao, Qianqian Zhang, Ruochen Xu, and Tiancheng Zhao. Vlm-r1: A stable and generalizable r1-style large vision-language model. *arXiv preprint arXiv:2504.07615*, 2025. 1

[71] Guangming Sheng, Chi Zhang, Zilingfeng Ye, Xibin Wu, Wang Zhang, Ru Zhang, Yanghua Peng, Haibin Lin, and Chuan Wu. Hybridflow: A flexible and efficient rlhf framework. *arXiv preprint arXiv: 2409.19256*, 2024. 5

[72] Chong Wang, Yuanhong Chen, Fengbei Liu, Yuyuan Liu, Davis James McCarthy, Helen Frazer, and Gustavo Carneiro. Mixture of gaussian-distributed prototypes with generative modelling for interpretable and trustworthy image recognition. *IEEE Transactions on Pattern Analysis and Machine Intelligence*, 2025. 1

[73] Han Wang, Yongjie Ye, Yanjie Wang, Yuxiang Nie, and Can Huang. Elysium: Exploring object-level perception in videos via mllm. In *European Conference on Computer Vision*, pages 166–185. Springer, 2024. 6

[74] Liuyi Wang, Xinyuan Xia, Hui Zhao, Hanqing Wang, Tai Wang, Yilun Chen, Chengju Liu, Qijun Chen, and Jiangmiao Pang. Rethinking the embodied gap in vision-and-language navigation: A holistic study of physical and visual disparities. In *Proceedings of the IEEE/CVF International Conference on Computer Vision*, pages 9455–9465, 2025. 1, 3

[75] Peng Wang, Shuai Bai, Sinan Tan, Shijie Wang, Zhihao Fan, Jinze Bai, Keqin Chen, Xuejing Liu, Jialin Wang, Wenbin Ge, et al. Qwen2-vl: Enhancing vision-language model's perception of the world at any resolution. *arXiv preprint arXiv:2409.12191*, 2024. 1, 2, 3, 6

[76] Weiyun Wang, Zhangwei Gao, Lianjie Chen, Zhe Chen, Jinguo Zhu, Xiangyu Zhao, Yangzhou Liu, Yue Cao, Shenglong Ye, Xizhou Zhu, et al. Visualprm: An effective process reward model for multimodal reasoning. *arXiv preprint arXiv:2503.10291*, 2025. 2

[77] XuDong Wang, Shaolun Zhang, Shufan Li, Konstantinos Kallidromitis, Kehan Li, Yusuke Kato, Kazuki Kozuka, and Trevor Darrell. Segllm: Multi-round reasoning segmentation. *arXiv preprint arXiv:2410.18923*, 2024. 6

[78] Eric Wiewiora. Potential-based shaping and q-value initialization are equivalent. *Journal of Artificial Intelligence Research*, 19:205–208, 2003. 2, 3

[79] Tim Windecker, Manthan Patel, Moritz Reuss, Richard Schwarzkopf, Cesar Cadena, Rudolf Lioutikov, Marco Hutter, and Jonas Frey. Navitrace: Evaluating embodied navigation of vision-language models. *arXiv preprint arXiv:2510.26909*, 2025. 1, 3

[80] Chenfei Wu, Jiahao Li, Jingren Zhou, Junyang Lin, Kaiyuan Gao, Kun Yan, Sheng ming Yin, Shuai Bai, Xiao Xu, Yilei Chen, Yuxiang Chen, Zecheng Tang, Zekai Zhang, Zhengyi Wang, An Yang, Bowen Yu, Chen Cheng, Dayiheng Liu, Deqing Li, Hang Zhang, Hao Meng, Hu Wei, Jingyuan Ni, Kai Chen, Kuan Cao, Liang Peng, Lin Qu, Minggang Wu, Peng Wang, Shuting Yu, Tingkun Wen, Wensen Feng, Xiaoxiao Xu, Yi Wang, Yichang Zhang, Yongqiang Zhu, Yujia Wu, Yuxuan Cai, and Zenan Liu. Qwen-image technical report, 2025. 1

[81] Jiannan Wu, Muyan Zhong, Sen Xing, Zeqiang Lai, Zhaoyang Liu, Zhe Chen, Wenhai Wang, Xizhou Zhu, Lewei Lu, Tong Lu, et al. Visionllm v2: An end-to-end generalist multimodal large language model for hundreds of vision-language tasks. *Advances in Neural Information Processing Systems*, 37:69925–69975, 2024. 3

[82] Zhuofan Xia, Dongchen Han, Yizeng Han, Xuran Pan, Shiji Song, and Gao Huang. Gsva: Generalized segmentation via multimodal large language models. In *Proceedings of the IEEE/CVF Conference on Computer Vision and Pattern Recognition*, pages 3858–3869, 2024. 3

[83] Huihui Xu, Yuanpeng Nie, Hualiang Wang, Ying Chen, Wei Li, Junzhi Ning, Lihao Liu, Hongqiu Wang, Lei Zhu, Jiyao Liu, Xiaomeng Li, and Junjun He. Medground-r1: Advancing medical image grounding via spatial-semantic rewarded group relative policy optimization. *arXiv preprint arXiv:2507.02994*, 2025. 3

[84] Cilin Yan, Haochen Wang, Shilin Yan, et al. Visa: Reasoning video object segmentation via large language models. In *ECCV*, 2024. 3

[85] Senqiao Yang, Tianyuan Qu, Xin Lai, Zhuotao Tian, Bohao Peng, Shu Liu, and Jiaya Jia. Lisa++: An improved baseline for reasoning segmentation with large language model. *arXiv preprint arXiv:2312.17240*, 2023. 5

[86] Shuo Yang, Yuwei Niu, Yuyang Liu, Yang Ye, Bin Lin, and Li Yuan. Look-back: Implicit visual re-focusing in mllm reasoning. *arXiv preprint arXiv:2507.03019*, 2025. 3

[87] Xianhang Ye, Yiqing Li, Wei Dai, Miancan Liu, Ziyuan Chen, Zhangye Han, Hongbo Min, Jinkui Ren, Xiantao Zhang, Wen Yang, and Zhi Jin. Gui-arp: Enhancing grounding with adaptive region perception for gui agents. *arXiv preprint arXiv:2509.15532*, 2025. 3

[88] Zhangyue Yin, Qiushi Sun, Zhiyuan Zeng, Qinyuan Cheng, Xipeng Qiu, and Xuanjing Huang. Dynamic and generalizable process reward modeling. *arXiv preprint arXiv:2507.17849*, 2025. 3

[89] Zuyao You and Zuxuan Wu. Seg-r1: Segmentation can be surprisingly simple with reinforcement learning. *arXiv preprint arXiv:2506.22624*, 2025. 1, 3, 6

[90] Licheng Yu, Patrick Poirson, Shan Yang, Alexander C Berg, and Tamara L Berg. Modeling context in referring expressions. In *European conference on computer vision*, pages 69–85. Springer, 2016. 2, 5, 6, 7

[91] Qiyuan Yu, Jue Liu, Xiaoyu Li, Yicheng Xu, Tianyi Zhang, et al. Dapo: Decoupled clip and dynamic sampling policy optimization for large language model reinforcement learning. *arXiv preprint arXiv:2503.14476*, 2025. 3

[92] Runpeng Yu, Xinyin Ma, and Xinchao Wang. Introducing visual perception token into multimodal large language model. *arXiv:2502.17425*, 2025. 3

[93] Xiang Yue, Tianyu Zheng, Yuansheng Ni, Yubo Wang, Kai Zhang, Shengbang Tong, Yuxuan Sun, Botao Yu, Ge Zhang, Huan Sun, et al. Mmmu-pro: A more robust multi-discipline multimodal understanding benchmark. *arXiv preprint arXiv:2409.02813*, 2024. 7

[94] Xiang Yue, Tianyu Zheng, Yuansheng Ni, Yubo Wang, Kai Zhang, Shengbang Tong, Yuxuan Sun, Botao Yu, Ge Zhang, Huan Sun, et al. Mmmu-pro: A more robust multi-discipline multimodal understanding benchmark. In *Proceedings of the 63rd Annual Meeting of the Association for Computational Linguistics (Volume 1: Long Papers)*, pages 15134–15186, 2025. 5, 6

[95] Yuhang Zang, Hanlin Goh, Josh Susskind, and Chen Huang. Overcoming the pitfalls of vision-language model finetuning for ood generalization. *arXiv preprint arXiv:2401.15914*, 2024. 3

[96] Jingyi Zhang, Jiaxing Huang, Sheng Jin, and Shijian Lu. Vision-language models for vision tasks: A survey. *IEEE transactions on pattern analysis and machine intelligence*, 46(8):5625–5644, 2024. 3

[97] Kaichen Zhang, Bo Li, Peiyuan Zhang, Fanyi Pu, Joshua Adrian Cahyono, Kairui Hu, Shuai Liu, Yuanhan Zhang, Jingkang Yang, Chunyuan Li, and Ziwei Liu. Lmms-eval: Reality check on the evaluation of large multimodal models, 2024. 6

[98] Wenbo Zhang, Tianrun Hu, Yanyuan Qiao, Hanbo Zhang, Yuchu Qin, Yang Li, Jiajun Liu, Tao Kong, Lingqiao Liu, and Xiao Ma. Chain-of-action: Trajectory autoregressive modeling for robotic manipulation. *arXiv preprint arXiv:2506.09990*, 2025. 1, 3

[99] Zhenru Zhang, Chujie Zheng, Yangzhen Wu, Beichen Zhang, Runji Lin, Bowen Yu, Dayiheng Liu, Jingren Zhou, and Junyang Lin. The lessons of developing process reward models in mathematical reasoning. *arXiv preprint arXiv:2501.07301*, 2025. 2, 3

[100] Enyu Zhao, Vedant Raval, Hejia Zhang, Jiageng Mao, Zeyu Shangguan, Stefanos Nikolaidis, Yue Wang, and Daniel Seita. Manipbench: Benchmarking vision-language models for low-level robot manipulation. *arXiv preprint arXiv:2505.09698*, 2025. 1

[101] Congming Zheng, Jiachen Zhu, Zhuoying Ou, Yuxiang Chen, Kangning Zhang, Rong Shan, Zeyu Zheng, Mengyue Yang, Jianghao Lin, Yong Yu, et al. A survey of process reward models: From outcome signals to process supervisions for large language models. *arXiv preprint arXiv:2510.08049*, 2025. 2, 3

[102] Guanghao Zhou, Panjia Qiu, Cen Chen, Jie Wang, Zheming Yang, Jian Xu, and Minghui Qiu. Reinforced mllm: A survey on rl-based reasoning in multimodal large language models. *arXiv preprint arXiv:2504.21277*, 2025. 3

[103] Yuqi Zhou, Sunhao Dai, Shuai Wang, Kaiwen Zhou, Qinglin Jia, and Jun Xu. Gui-g1: Understanding r1-zero-like training for visual grounding in gui agents. *arXiv preprint arXiv:2505.15810*, 2025. 3

[104] Deyao Zhu, Jun Chen, Xiaoqian Shen, Xiang Li, and Mohamed Elhoseiny. Minigpt-4: Enhancing vision-language understanding with advanced large language models. *arXiv preprint arXiv:2304.10592*, 2023. 1, 2

[105] Jinguo Zhu, Weiyun Wang, Zhe Chen, Zhaoyang Liu, Shenglong Ye, Lixin Gu, Hao Tian, Yuchen Duan, Weijie Su, Jie Shao, et al. Internvl3: Exploring advanced training and test-time recipes for open-source multimodal models. *arXiv preprint arXiv:2504.10479*, 2025. 2, 3